Energetics and Kinetics of Radical Pairs in Reaction Centers from *Rhodobacter sphaeroides*. A Femtosecond Transient Absorption Study[†,‡]

A. R. Holzwarth* and Marc G. Müller

Max-Planck-Institut für Strahlenchemie, Stiftstrasse 34-36, D-45470 Mülheim a.d. Ruhr, Germany

Received March 22, 1996; Revised Manuscript Received June 17, 1996[⊗]

ABSTRACT: Femtosecond transient absorption spectra on reaction centers from *Rhodobacter sphaeroides* wild type have been recorded with high time and wavelength resolution and a very high S/N ratio in the 500−940 nm range with a diode array system. The data have been analyzed by global analysis. Five lifetime components of 1.5, 3.1, 10.8, and 148 ps and long-lived (several nanoseconds) were required to fit the entire three-dimensional data surface adequately with a single set of lifetimes and decay-associated difference spectra (DADS). Up to 30 ps, there is little dispersion in the lifetimes, but in the longer time range (50−250 ps), a substantial variation in lifetime was observed, depending on detection wavelength. The data from the global analysis have been subjected to kinetic modeling comparing sequential kinetic schemes either including (reversible model) or excluding (forward model) back-reactions in the early electron transfer process(es). Thus, the molecular rate constants for the model(s) and the difference spectra of the pure intermediates [species-associated difference spectra (SADS)] were obtained. The data unequivocally confirm the necessity of an electron transfer intermediate with spectral characteristics of P^+B^-H prior to the formation of the P^+BH^- state (P is special pair, B is accessory chlorophyll, and H is pheophytin), irrespective of the model chosen. Besides being in much better agreement with the observation of long-lived fluorescence kinetics components, the reversible model results in SADS, in particular for the P^+BH^- state, that are in somewhat better agreement with expectations than for the pure forward model. For these and other reasons, the reversible model is preferred over the pure forward model. The electrochromic shifts of the H bands in the P^+B^- state and of the B bands in the P^+H^- state are revealed clearly in the spectra, thus supporting the assignments. Within the reversible model, the rate constant for the forward reaction in the first step $P^* \rightleftharpoons P^+B^-H$ is slightly larger [$k_{12} \approx (2.48\ \text{ps})^{-1}$] than for the second step $P^+B^-H \rightleftharpoons P^+BH^-$ [$k_{23} \approx (2.53\ \text{ps})^{-1}$], in contrast to the pure forward model. From the rate constants for the respective back-reactions, the free energy differences ΔG relative to P* for the states P^+B^-H and P^+BH^- have been determined to be −41 and −91 meV, respectively. Thus, the free energy difference for the P^+BH^- state at early times after electron transfer is by a factor of 2−3 smaller than assumed so far. This has the important consequence that a quasi-equilibrium exists from about 10 ps until further electron transfer on the 200 ps time scale with a substantial percentage (≈16%) of the P^+B^-H state present. These results present the first direct evidence from transient absorption data, where the nature of the intermediate can be assigned, for the validity of the slow radical pair relaxation concept. The results have various consequences for understanding the mechanism of the overall electron transfer reaction and imply a much more active role of the protein in the early charge separation processes of the reaction center than assumed so far. The data are discussed in terms of current electron transfer theory. It is suggested that the two first-electron steps operate at a rate very close to the maximal possible rate.

In photosynthesis, the conversion of light energy into chemical energy occurs by a series of photoinduced electron transfer processes across membrane-bound pigment−protein complexes, the so-called reaction centers (RCs).[1] Due to the variety of different electron transfer reactions in RCs, ranging from picoseconds to seconds, these systems have become model systems for the study of electron transfer processes in proteins in recent years (Parson, 1991; Moser et al., 1993). Although the overall process of charge separation in bacterial RCs is quite well-understood, the detailed mechanism of the early step(s) and their possible theoretical explanations are still discussed very controversially (Kirmaier & Holten, 1991; Arlt et al., 1993; Jia et al., 1993).

The photoinduced electron transfer in RCs starts from a so-called "special pair" P* (an excited bacteriochlorophyll dimer). The other electron transfer cofactors present in the bacterial RC are arranged in two nearly *C*2-symmetric branches (called A and B branches, from which only A is

[†] Partial financial support has been provided by the Deutsche Forschungsgemeinschaft (Sonderforschungsbereich 189, Heinrich-Heine-Universität Düsseldorf and Max-Planck-Institut für Strahlenchemie, Mülheim a.d. Ruhr).

[‡] A preliminary account of this work has been presented at the conference on "Ultrafast Processes in Spectroscopy, Trieste, Italy, October 1995 (Müller & Holzwarth, 1995).

* Corresponding author. Fax: (+49) 208 306 3951. E-mail: Holzwarth@mpi-muelheim.mpg.de.

[⊗] Abstract published in *Advance ACS Abstracts,* August 1, 1996.

[1] Abbreviations: (bacterio)-Chl, (bacterio)-chlorophyll; (bacterio)-Pheo, (bacterio)-pheophytin; RC, reaction center; DADS, decay-associated difference spectra; SADS, species-associated difference spectra; ET, electron transfer; P, reaction center special pair; B, accessory bacteriochlorophyll; H, bacteriopheophytin; RP, radical pair; λ, reorganization energy for electron transfer; V, electronic coupling matrix element for electron transfer.

S0006-2960(96)00701-5 CCC: $12.00

active), each containing a monomeric (accessory) bacteriochlorophyll (B), a bacteriopheophytin (H), and a quinone (Q). It has been known for quite some time that the electron arrives on H of the A branch in about 3 ps time and continues to Q_A (the quinone in the active A branch) with a time constant of about 200 ps [see Parson (1991) for a review]. In principle, two alternative extreme mechanisms can be envisaged for the transfer to H: (i) a sequential mechanism involving P^+B^- as a real intermediate and (ii) a so-called superexchange mechanism where B provides a virtual state only for the ET but is not present as a real B^- intermediate and the electron goes directly to H (Marcus, 1987). While early experimental work preferred the superexchange mechanism (Kirmaier et al., 1985b; Woodbury et al., 1985), Zinth and co-workers in a series of papers have provided evidence that strongly supports the first possibility, i.e. B^- as a real intermediate in a reaction scheme

$$XP^* \xrightarrow{k_1} B \xrightarrow{k_2} H$$

with $k_2 > k_1$ (Arlt et al., 1993; Holzapfel et al., 1989, 1990). In the kinetic scheme used by Zinth and co-workers, $1/k_1 \approx 3.5$ ps and $1/k_2 \approx 0.9$ ps. Despite the substantial amount of data favoring the sequential mechanism, it is nevertheless not generally accepted, however. One of the various reasons why this sequential model is still considered with a skeptical attitude by a number of researchers is the fact that on the fast time scale of a few picoseconds other processes may occur as well or compete with ET. These are, e.g., coherent vibrational motion in the excited state (Vos et al., 1991, 1994) and early protein dynamics (Peloquin et al., 1994; Müller et al., 1995), which may well complicate the situation. In addition, it is now well-known that the actual decay kinetics of P* is much more complex than expected even on the basis of the sequential mechanism. For example, substantial amplitudes of a ca. 10−15 ps component have been observed in the spontaneous and stimulated emission from P*, the origins of which are quite uncertain at present (Müller et al., 1992, 1995; Wang et al., 1993; Du et al., 1992; Hamm et al., 1993). Thus, static protein conformations, giving rise to a dispersive kinetics of the P* decay in the primary ET step, have been invoked as one explanation (Du et al., 1992; Jia et al., 1993; Bixon et al., 1995). Another possibility would be a dynamic solvation of the radical pair(s) which could report back to the P* state via a radical pair recombination process (Müller et al., 1992, 1995; Woodbury et al., 1994; Peloquin et al., 1994). In any case, it is clear that either static or dynamic protein conformational states have a substantial influence on the early electron transfer step(s). Unless the source of this dispersive kinetics is revealed, we do not have a sound understanding of the mechanism of the early photosynthetic ET process(es) and its interplay with protein states and motions in this complex system. One of the possibilities that has much attraction for an explanation of many of the so far unexplained deviations from exponential kinetics is a more active role of the protein in the overall electron transfer process than anticipated so far.

From a theoretical point of view, the energetics of the radical pair states, besides their kinetics, is of utmost importance for the understanding of the ET process. In particular, the energy of the (real or virtual) P^+B^-H and the P^+BH^- states relative to P* is a decisive factor in the theoretical decision on the mechanism, i.e. sequential vs superexchange. Theoretical calculations within their accuracy limit could not provide a clear-cut answer and resulted in energy differences from several hundred to about 1000 cm^{-1} above to about 500 cm^{-1} below P* for the P^+B^-H state (Creighton et al., 1988; Parson et al., 1990). The most recent calculations (Alden et al., 1995) put the energy of P^+B^-H about 1000 cm^{-1} below P*, with an ≈1000 cm^{-1} error, and the P^+BH^- state about 2300 cm^{-1} below P*. Recent theoretical modeling, taking into account a variety of experimental data, now gives preference to a dominance of the sequential mechanism, at least at temperatures near room temperature (Bixon et al., 1995). These conclusions are based, however, on a number of assumptions that are not sufficiently well-tested experimentally at present. For example, for the sequential scheme, no clear energetics of the first radical pairs in the native system is known, although an attempt has been made to estimate this number using a chemically modified RC (Schmidt et al., 1994), resulting in $\Delta G \cong -450$ cm^{-1} for the first step in that modified RC. Furthermore, the theoretical kinetic modeling ascribes the nonexponentiality entirely to a distribution of ΔG values in the first and second ET steps derived from a static distribution of RP energies (Bixon et al., 1995). This leads to a large rate distribution for the primary step of about 3 orders of magnitude. While quite attractive, this assumption remains to be tested by experiment.

The situation seems to be more clear with respect to the free energy difference of the second RP, i.e. the P^+BH^- state relative to P*. Direct triplet spectroscopy (Boxer et al., 1988) and MARY spectroscopy (Goldstein et al., 1988; Chidsey et al., 1985; Ogrodnik et al., 1988, 1994) resulted in a ΔG value of approximately −1600 to −2000 cm^{-1} relative to P* and an energetic width of about 400 cm^{-1} due to (static) heterogeneity (Ogrodnik et al., 1994). These numbers are however in vast conflict with results based on recombination fluorescence which repeatedly showed that radical pairs exist at room temperature with free energy differences on the order of several hundred cm^{-1} to P* (Woodbury & Parson, 1984; Peloquin et al., 1994; Müller et al., 1992, 1993, 1995) at high temperatures near room temperature and even much smaller values at low temperatures (Woodbury et al., 1994; Peloquin et al., 1994). Similarly small ΔG values are also known from photosystem II reaction centers (Booth et al., 1990, 1991; Roelofs et al., 1991; Müller et al., 1996; Konermann et al., 1996; Gatzen et al., 1996). Until this discrepancy is resolved, the free energy difference of the P^+BH^- state must be considered uncertain. Clearly, the disadvantage of the recombination fluorescence measurements is that the chemical identity of the RP states cannot be identified, although the presence of such high-energy RP states seems to be well-documented from these results.

In their early papers proposing the sequential mechanism, Zinth and co-workers employed a pure forward reaction scheme (Arlt et al., 1993), thus implying large energy differences of several times the thermal energy kT for the pairs P^*/P^+B^-H and P^+BH^-/P^+B^-H. Since it has been known for quite some time that charge recombination fluorescence occurs with relative amplitudes of a few percent or more, depending on which of the components slower than about 3−4 ps are attributed to this process, a pure forward reaction scheme seems to be inadequate to properly describe the early processes (Müller et al., 1992, 1995; Woodbury &

Parson, 1986; Woodbury et al., 1994). This follows also from the work on the chemically modified RC (Schmidt et al., 1994). Little is known from direct femtosecond experiments for the energy difference of the second step P^+B^-H/P^+BH^-, and it is thus desirable that the energetics of the first radical pairs, as well as other parameters, be directly determined in the wild-type RC. This should indeed be possible, provided that kinetic data with a sufficiently high S/N ratio are available. Then alternative kinetic schemes could be tested on these data sets. It is important to note that the kinetic analysis not only must provide a satisfactory description of the kinetics but also must, at the same time, provide physically reasonable (transient) spectra and eventually result in an integrated approach within the same kinetic model that explains both transient absorption and fluorescence and possible other data as well. Quite importantly, a satisfactory model must also explain the dispersive kinetics (Müller et al., 1992), the temperature and redox dependence of the kinetics, and energetics of the RP states at the same time. This aim has not been achieved so far, and it will probably not be possible to achieve it in a single try. Furthermore, a satisfactory model should also give some clues toward an understanding of the intricate interaction with and dependence of the kinetics on the protein dynamics and the possible role of various alternative mechanisms proposed recently (Skourtis et al., 1992; Woodbury et al., 1994; Müller et al., 1992). Within this general long-term goal, the present paper has two aims: (i) to further test the evidence for a P^+B^- state and the sequential model (including back-reactions) on the basis of a complete set of high S/N ratio femtosecond transient spectra and (ii) to try to determine the rate constants and RP energies within that scheme. The necessary experimental basis will be a well-resolved transient absorption data set over a wide range of detection wavelengths and a very high S/N ratio on wild-type RCs.

MATERIALS AND METHODS

Reaction centers from wild-type *Rhodobacter sphaeroides* (Deutsche Sammlung von Mikroorganismen, Braunschweig) were isolated as described (Müller et al., 1992) and were subjected to further HPLC purification. For measurements, the samples were prepared at an OD $\approx$ 1/mm at 800 nm in a rotating cuvette which was also shifted periodically (1/s) in a horizontal direction. Thus, the time between hitting the same sample volume a second time was $\geq$20 s on average. All measurements were carried out at room temperature ($\approx$23 °C). Femtosecond transient spectra and kinetics were recorded with a laser system described previously (Müller et al., 1996). In brief, femtosecond excitation pulses were generated by chirped pulse amplification of 40 fs pulses from a Ti-sapphire laser oscillator (Tsunami, Spectra Physics) in a regenerative amplifier and stretcher/compressor unit (Quantronix). The output pulses from the amplifier (FWHM = 70−80 fs) were frequency-shifted using an optical parametric generator (Topas, Light Conversion) whose output pulses (60−70 fs FWHM) were close to being transform-limited. Part of the 800 nm light from the amplifier was used to generate a white light continuum with an $\approx$80 fs width (FWHM). The pump and white light probe pulses were polarized at magic angle relative to each other in order to exclude any kinetic depolarization effects. The detection system was a spectrograph/diode array system. Three-dimensional Δabsorption/time/wavelength data sets were recorded with various time resolutions per step and over different time ranges. The rms noise of the detection system was about $\pm 5 \times 10^{-5}$ OD units under actual measurement conditions in most wavelength ranges. A low photon density of 1.2×10^{14} photons per cm^2 per pulse (repetition rate of 3 kHz) was applied for excitation at 860 nm (13 nm FWHM), which bleached about 5% of the RC P860 absorption band.

Data were analyzed in a global fashion by combining the data sets recorded at all detection wavelength pairs and at two or three different time resolutions and time ranges over which the data have been measured (equal weighting of the various ranges). In this way, decay-associated difference spectra (DADS) and a global set of lifetimes have been obtained (Holzwarth et al., 1993; Holzwarth, 1996). The global analysis included a deconvolution of the kinetics with the autocorrelation of the excitation pulse, although this was not absolutely required for resolving lifetimes above 200 fs in view of the very narrow excitation pulse. The global lifetime analysis was performed with linked lifetimes and, quite importantly, linked amplitude ratios for the data from the different measuring time ranges (Holzwarth, 1996). This is required in order to get a unique lifetime/DADS data set from the different time ranges. In addition, global target analysis has been performed on the output from the combined global analysis (lifetimes and DADS) in order to test various kinetic models. This involves a simultaneous optimization of the rate constants and the spectra in order to optimally describe the input data. The results of this analysis are the rate constants of the model chosen and the so-called species-associated difference spectra (SADS) of each species or intermediate present in the model (Holzwarth et al., 1993; Holzwarth, 1996). For further details, the reader is referred to Holzwarth (1996) which describes the various methods in detail. The approach of performing the kinetic modeling on the DADS and lifetimes rather than on the original decay data is advantageous here since it is more flexible and much less computer-time consuming.

RESULTS

Femtosecond transient spectra were recorded with the camera system in wavelength intervals of 120 nm in a single run. The detection wavelength ranges chosen were 520−640, 620−740, 700−820, and 790−910 nm at a spectral resolution of 0.5 nm. Furthermore, the 930−960 nm range has been measured for a precise determination of the stimulated emission (see below). For each interval, two, or sometimes three, time ranges (or resolutions) were recorded, i.e. 0−20, 0−200 or 0−300, and 0−700 ps. A large detection time range is required in order to reliably allow, from the same data set, the analysis of the expected time constants ranging from subpicoseconds to several nanoseconds (nondecaying component). An example of one of the original three-dimensional data surfaces is shown in Figure 1 for a detection wavelength range of 520−640 nm and a 20 ps time range. Of particular interest in this figure is the very fast bleaching ($\approx$1 ps) near 540 nm which will be identified below as an electrochromic shift.

Combined and amplitude-linked (see above) global lifetime analysis of all data sets indicated that five lifetimes were generally required to describe the entire data surface for all wavelengths. Since the fast lifetimes can only be determined accurately from the high time resolution data sets, while the

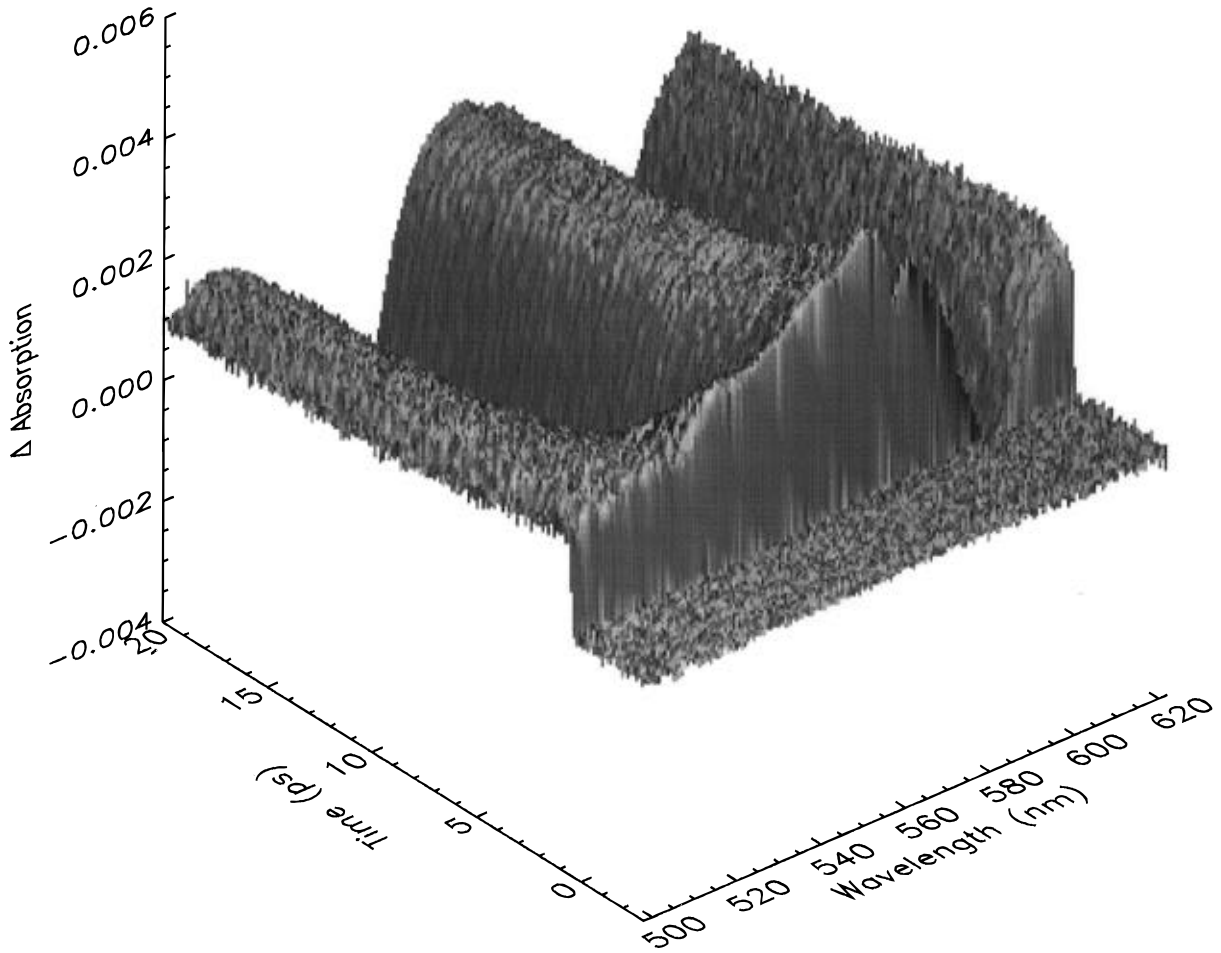

FIGURE 1: Three-dimensional data surface from femtosecond transient absorption measurements ($\lambda_{exc} = 860$ nm) on wild-type *Rb. sphaeroides* RCs. The wavelength range was 500−540 nm; the time range was 20 ps, and $T = 23$ °C.

accurate determination of the long lifetimes requires a large time range, the various time range data sets were linked in the analysis in such a way that the set of lifetimes was the same (but freely variable) and the amplitude ratios (not the absolute amplitudes) of the components were the same for each time range. In this way, a unique solution describing well all the various time ranges can be found. The optimal set of global lifetimes was as follows: $\tau_1 = 1.5 \pm 0.2$ ps, $\tau_2 = 3.1 \pm 0.2$ ps, $\tau_3 = 147 \pm 15$ ps, $\tau_4 =$ nondecaying several nanoseconds (any value above 4 ns gave an equally good fit), and $\tau_5 = 10.8 \pm 1$ ps. Note that the errors indicated are the statistical errors of the global analysis. They do not reflect any systematic wavelength dependencies that may exist (see below). The results from the combined (all wavelengths and time ranges) and amplitude-linked global analysis are shown in panels A and B of Figure 2 as DADS. This set of DADS and lifetimes resulted in a very good fit over the whole three-dimensional data surfaces except for a few wavelengths where the fit is suboptimal. Around the excitation wavelength of 860 ± 30 nm, an additional ultrafast component with a lifetime on the order of the pulse length was required in order to avoid a sharp spike in the residuals of the kinetic fits. This component was fixed to 0.1 ps in the analysis. It may have various origins, ranging from pure artifact, but more likely arises from coherent effects. Its amplitude was very small or absent far away from the excitation wavelength. Within the framework of this paper, we will not consider this component any further and treat it as a pure mathematical fitting parameter without giving it any physical interpretation. For this reason, it will also not be shown in the DADS presented below. It is important to note, however, that the lifetime of the fastest component would be reduced significantly if this ultrafast component were not accounted for by an additional lifetime.

The $\tau_5 = 10.8$ ps component had generally also quite a low (less than 2−3%) amplitude except in the wavelength ranges near 540 nm, around 760 nm, and above 820 nm where the amplitude was larger, ranging up to 5−10% of the total. The spectral shape of this component resembles closely the shape of the $\tau_2 = 3.1$ ps component, although there are also deviations present. Its lifetime is clearly reminiscent of the 10−15 ps component observed first in fluorescence (Müller et al., 1991, 1992; Du et al., 1992). Although the presence of this component has been observed at a few individual wavelengths before also in transient absorption (mostly around 920 nm), its full difference spectrum has not been reported before. This component cannot be left out of the analysis in most wavelength ranges if one aims at a good fit. This component is shown only in the DADS, but we will ignore it in the discussion and further analysis for the purpose of the present paper, notwithstanding the well-established fact that it arises from native RCs and will eventually have to be included at a later stage of more refined kinetic modeling, in particular when trying to arrive at a detailed description of the dispersive kinetics.

In view of previous reports on the wavelength dependence of the lifetimes, we also performed a separate global analysis over more limited wavelength ranges. Some wavelength

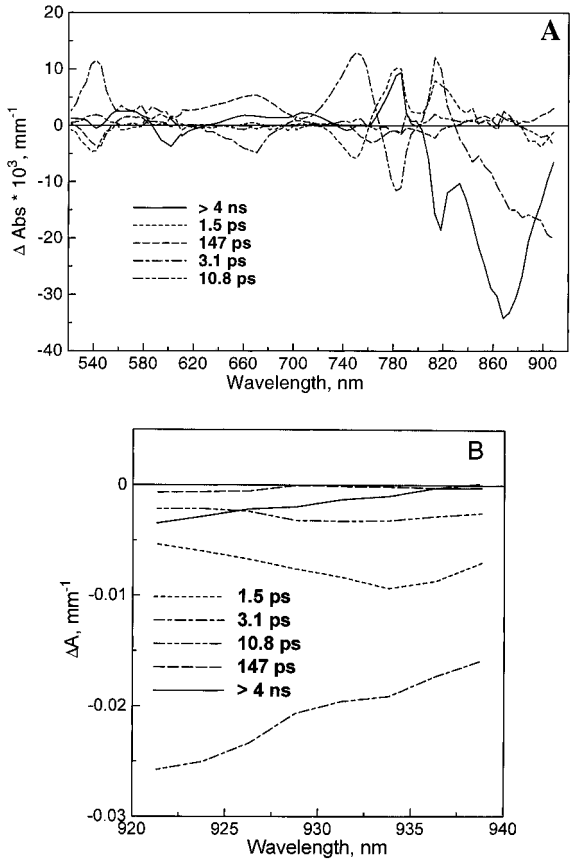

FIGURE 2: DADS from combined global analysis of all decays taken in different wavelength and time ranges. **Note for Figures 2, 3, and 5:** In the wavelength range 800 ± 7 nm, the amplitudes may be partially distorted due to the fact that $\lambda = 800$ nm has been used as the generating wavelength for the white light continuum: (A) full spectrum of 520−910 nm and (B) extended long-wavelength range for determination of stimulated emission.

dependence of the lifetimes was found (not shown), but it was relatively small for the lifetime components τ_1 (1.0−1.6 ps) and τ_2 (2.9−3.5 ps); this dependence might be explained to a substantial degree by increased statistical errors alone if the global analysis is performed over a more limited number of wavelengths, as compared to global analysis across the entire range. However, lifetime component τ_3 (147 ps) varied substantially more from about 60 to 300 ps when the analysis was performed over different wavelength ranges. Thus, subject to more stringent future checks, one has to be aware that to some extent all lifetime components may show some modest distribution, but the relative width of such a distribution will certainly be by far largest for the τ_3 component. Nevertheless, within a good accuracy, the whole data surface can be described very well within the single set of lifetimes given above, with the exception of a few wavelengths only where the fitting was suboptimal. This set of global lifetimes will be used together with the corresponding DADS as a basis for the kinetic analysis irrespective of any possible (small) distributions. Similar data have been obtained also with R26 RCs (data not shown).

Figure 3 gives the transient spectra at various delay times for better comparison with published data. The spectra shown have actually been recalculated from the DADS and the lifetimes. We prefer this presentation over the directly measured spectra since these recalculated spectra are already corrected for some artifacts like, e.g., the time dispersion across the wavelength range and baseline offsets. They agree

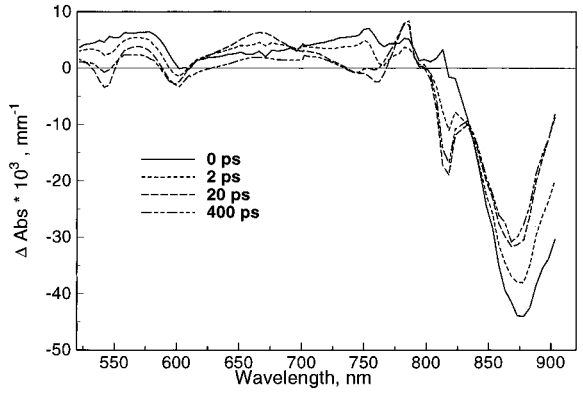

FIGURE 3: Absorption difference spectra at various delay times. The spectra shown have been recalculated from the DADS shown in Figure 2 and are thus corrected for the time dispersion and for any existing baseline offsets. See the note in Figure 2.

very well with the directly measured spectra if these corrections are taken into account, however.

DISCUSSION

The data presented in Figure 2 clearly indicate that two ultrafast phases of about 1.5 and 3.1 ps are required to fit the data in a sum of exponentials modeling in almost all wavelength ranges. The following kinetic modeling of the ET processes will take into account all the lifetimes and DADS (Figure 2) obtained from the combined global analysis except for the $\tau_5 = 10.8$ ps component. For the time being, the latter component is considered here as a (small) perturbation of the overall kinetics whose precise origin is difficult to locate at present. It could be due to some distribution in the early ET rates (Müller et al., 1992, 1995; Wang et al., 1993; Jia et al., 1993), but it could also be due to entirely different reasons (see discussion below). In view of the rather small amplitudes of this component, we believe that the systematic error exerted on the results of the kinetic modeling by not considering this component in a first-order model will be small.

Possible Lifetime Distributions and Wavelength Dependence. The systematic wavelength dependence of the lifetimes reported by Kirmaier and Holten (1990) for the short lifetimes is well accounted for in our data by the resolution of their ≈3 ps component into 3.1, 1.5, and 10.8 ps components. That wavelength dependence, though in a single-exponential description, is thus confirmed by our measurements, but it is now resolved into three discrete lifetimes. The previous wavelength dependence of a single lifetime can be understood well now in terms of the mixing of these lifetimes. Our analysis suggests that any remaining systematic wavelength dependence in this short time range seems to be quite small (see above). This is not the case for the longer time range of 50 ps to several hundred picoseconds, where a similar wavelength dependence as reported already by Kirmaier and Holten (1990) is present in our data if analyzed on a single wavelength or narrow wavelength range basis (not shown). Since the DADS of the τ_3 component is substantially different for example from the corresponding DADS of the τ_2 component, which represents directly the main part of the P* decay, it is considered unlikely that any substantial contribution, to e.g., the τ_4 lifetime component (and its distribution or wavelength dependence) might arise from such slow P* decay of 100−

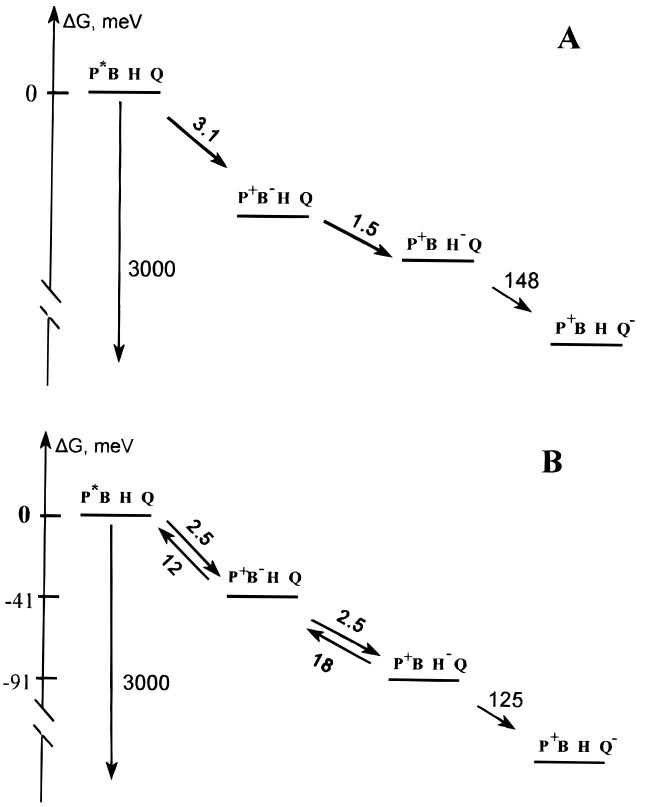

FIGURE 4: Kinetic models and their optimal inverse rate constants (picoseconds) as obtained by target analysis of the DADS and lifetimes from Figure 2: (A) forward model and (B) reversible model, including free energy differences.

200 ps. Such an interpretation more likely applies to the τ_5 component which shows much more similarity in its spectrum to that of the τ_2 component (Figure 2A). The current interpretation of this component involves indeed a nonexponentiality in the kinetics of the primary electron transfer process due to some kind of heterogeneity (Jia et al., 1993; Du et al., 1992). Since it is not the main aim of this paper to analyze in detail the possible distribution in lifetimes, it may suffice here to note that our data suggest that any distribution in the lifetimes analyzed here seems to be relatively small, i.e. by 1−2 orders of magnitude smaller than the rather wide distribution of the P* decay rates predicted by the recent theoretical work of Bixon et al. (1995). Rather, our data seem to suggest that one or more steps in the overall electron transfer process might have some modest distribution in rate, if any. In this paper, we will not address this problem any further. Rather, we will go on to explore the kinetics in a first approximation in terms of straightforward first-order rate equation models. The main motivation for the rate equation approach is (i) to further test the suggestion of a B^- intermediate and (ii) to determine the free energy differences for the radical pairs directly from the kinetics of the wild-type RC.

At this point, a remark on the kinetic analysis of transient absorption data is required. In the general case, the reversible kinetic model (Figure 4B) does not allow a unique solution on the basis of transient absorption data alone. This is because too many (in this case five) unknown rate constants are to be determined. Thus, the rates and also the SADS will be parametrically dependent upon each other. This dwells on the so-called identifiability problem in kinetic analysis (Holzwarth, 1996). In particular cases, a unique solution can nevertheless be obtained. For example, all rate constants in Figure 4B (except for the radiationless decay to ground state from P*) can be determined unequivocally on the basis of fluorescence lifetime data. Thus, if the analysis of the transient absorption data could be linked to fluorescence lifetime data, a unique solution can be found for the rate constants and also the SADS of the transient absorption data. So far, fluorescence measurements have not resolved the fastest component of about 1−1.5 ps, however (Müller et al., 1992; Jia et al., 1993; Hamm et al., 1993). The reason is that single-photon timing has an insufficient time resolution (Müller et al., 1992) and fluorescence up-conversion has an insufficient S/N ratio so far (Jia et al., 1993; Hamm et al., 1993) to resolve a small contribution of an about 1 ps component along with a dominant 3 ps component. However, the fact that up-conversion resulted in a generally shorter lifetime of the fastest component than transient absorption measurements may be taken as an indication that a small contribution of an $\sim$ 1 ps component is present in the spontaneous emission decay.

In the absence of any highly resolved spontaneous emission decay, the same purpose can be achieved however using the stimulated emission decay, provided a wavelength can be found where the absorption difference spectra of all radical pairs are zero, i.e. if they do not contribute to the signal in that region. This seems to be the case for bacterial RCs in the 910−950 nm range. We have thus measured carefully the transient absorption kinetics in this range (Figure 2B). We have then performed the complete target analysis for a variety of wavelengths in the 900−960 nm range, assuming that for that particular wavelength the above condition was satisfied. The second important requirement was that the observed kinetics in transient absorption should be in agreement with the spontaneous fluorescence results. Comparison of all the resulting data indicated that at 935 $\pm$ 2 nm both conditions are fulfilled quite well, i.e. the difference spectra of all radical pairs should have a zero crossing within the error limits. Thus, the transient absorption signal at this wavelength can be taken as a pure stimulated emission signal, with the same amplitude ratios of lifetime components as would be obtained in a spontaneous fluorescence measurement. In our data (Figure 2B), the largest component is the 3.1 ps one. The second largest component is the 1.5 ps component. Also, the 10.8 ps component has a substantial amplitude. The amplitude of the 147 ps component is also negative but very small ($\approx$2−3% of the amplitude of the 3.1 ps component). The accuracy in the amplitude determination of this latter long-lived component is thus not sufficient from the transient absorption data for the precision required for our analysis. However, since the long-lived component is very well-determined in the spontaneous emission, we have taken the relative amplitude of this component from our time-resolved fluorescence data (Müller et al., 1992, 1995). The amplitude in fluorescence is 2.6 $\pm$ 0.2% of the 3 ps component. Incidentally, the amplitude ratio of the 3.1 ps to the 10.8 ps component (6.3/1) in transient absorption is in very good agreement with that ratio in spontaneous fluorescence (6.6/1) (Müller et al., 1992). This represents actually an internal consistency check for the validity of the procedure. We thus have an amplitude ratio of 0.87/1.74/0.27/0.067 for the 1.5 ps/3.1 ps/10.8 ps/147 ps components. If this amplitude ratio of fluorescence is linked

to the analysis of the transient absorption data when analyzing Figure 4B, it allows a unique (for rates and SADS) solution of the kinetic model (note that in the following analysis the 10.8 ps component will be ignored).

Kinetics of Radical Pairs. In their first papers providing evidence for a B^- intermediate, Zinth et al. used a pure sequential forward reaction model to analyze their data, thus implying a relatively large energy gap of several times *kT* between the various intermediates. There is substantial evidence however against the validity of a pure forward reaction scheme in RCs. Thus, the substantial charge recombination fluorescence (Woodbury & Parson, 1984; Horber et al., 1986) indicates the presence of radical pairs with energy gaps to P* within 1−2 times *kT*. Recent reports of components with several tens of picoseconds would imply, if explained by charge recombination, the presence of such radical pairs with small energy gaps (Müller et al., 1992; Peloquin et al., 1994). We have thus tested the two extreme kinetic schemes against our data: a pure sequential forward model (Figure 4A) and a reversible model (Figure 4B). Reversible kinetics for only one of the first two reaction intermediates has also been tested but does not seem to be a reasonable possibility (results not shown). The main question here is whether these models can actually be distinguished clearly on the basis of the kinetic scheme and the species-associated spectra (SADS). At this instance, we make no a priori assignment of an actual chemical intermediate to any of the formal states in the kinetic models, except for the initial P* state which is directly excited by the laser pulse. Panels A and B of Figure 5 show the resulting SADS which result from the simultaneous optimization of rate constants and spectra for the two kinetic models.[2]

The optimal rate constants for the two models, as obtained from the fitting and kinetic modeling of the DADS, are also given in panels A and B of Figure 4. The forward model, gives rate constants that are essentially the inverse of the lifetimes, as expected for formal kinetic reasons. In the forward model the rate constant for the second step is larger than for the decay of the P* state, in full agreement with the result of Zinth and co-workers. In view of the longer fastest lifetime (1.5 ps in our data vs 0.9 ps in Zinth's work), the rate constant in the forward model for the second step (Figure 4A) is smaller as compared to Zinth's data and is only about by a factor of 2 larger than that for the first step. The 1.5 ps lifetime of this component in our data is mainly determined from the 520−620 and 740−790 nm ranges, while in the long wavelength range (above 800 nm), when fitted alone, the lifetime is ≈1.1 ps, i.e. closer to the value reported by Zinth et al. We note that in that long-wavelength range some fast-decaying coherent effects are present in the signal that shorten the fast lifetime to some extent, however (M. G. Müller and A. R. Holzwarth, to be published).

Comparison of the optimal rate constants for the pure forward and the reversible model shows some remarkable differences. First, the rates for the reverse reaction for both

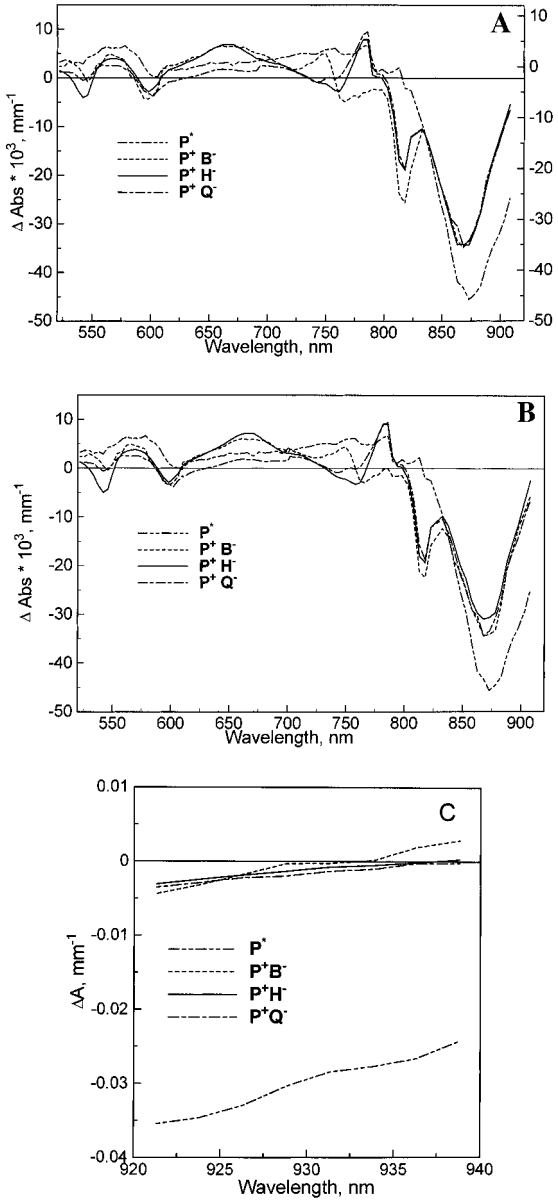

FIGURE 5: SADS calculated from the DADS in Figure 2 for the two kinetic models shown in Figure 4: (A) forward model, (B) reversible model (see the note in Figure 2), and (C) reversible model, long-wavelength range.

early steps are not negligible relative to the forward rates. Thus, the ratio k_{forw}/k_{rev} is 5/1 for the first step and somewhat higher, i.e. 7/1, for the second step. This means that none of the back-reactions can be ignored and that the reversible model is much more than a small correction to the pure forward model. In particular, the relatively high rate of the reverse reaction in the second step is very surprising given most current ideas about this reaction and its energetics. Furthermore, both forward rates are quite similar to each other, in contrast to the pure forward model.

We have noted above that for formal kinetic reasons a pure forward model should be able to mathematically describe the kinetics well. This is indeed found in the model fitting, i.e. the fit quality for the pure forward model is not substantially worse than the one for the reversible model. The models should differ in general in the shape of the SADS, however, and these differences should be more pronounced the larger the reverse rate in a step is in relation to the forward rate. Thus, a distinction between the models

[2] Note that it can be shown by formal kinetics that in a rate equation model the purely sequential forward model will always give a good description to the kinetics as long as the number of lifetimes is equal to the number of states in the kinetic model. The reversible model is an extension of the simplest possible model that formally will fit the kinetics. The distinction of which model is more appropriate can thus only be made on the basis of a decision about whether the corresponding SADS are physically reasonable for a particular model.

and a decision which is the one that is more appropriate for the RC should also be made on the basis of the resulting SADS which will now be compared in detail. Note in this connection the SADS for the reversible model in the long-wavelength range (Figure 5C) which are essential for our analysis. The spectra of all radical pairs have their zero crossing at 935 ± 2 nm.

The SADS of the initial P* state do not differ at all between the two models (Figure 5A,B) as required already for formal reasons since the initial state must be the same in both models. The spectra for the P* state found here agree very well with the spectra published earlier by other groups for early times (Kirmaier et al., 1985a; Woodbury et al., 1985) and with the SADS of Holzapfel et al. (1990). The SADS of the first intermediate (P^+B^-) are quite similar for the two kinetic models as well and show only some small overall amplitude differences of <10% but no distinct differences in the spectral features at any wavelength. The SADS for the first intermediate are characterized by a bleaching of the P band at 869 nm, a narrow bleaching at 813 nm,[3] a dispersive shape around 760 nm, a bleaching band at 599 nm and another dispersive shaped band at 543 nm. The two dispersive shapes seem to derive from electrochromic shifts in the Q_y and Q_x bands of H at 760 and 543 nm, respectively, due to the presence of the nearby B^-. The 813 nm bleach must be partly due to a bleaching of the B_A band. The 813 nm bleaching intensity, though slightly larger in the reversible model as compared to the bands of the other species than in the sequential forward model, appears to be somewhat small. Even if one takes into account some broad background absorption increase at this wavelength due to P^+, the bleaching band of a pure B^- state would be expected to be somewhat larger. We cannot make a strong point out of observation since (i) the spectra may be distorted substantially due to intensity redistribution caused by breaking exciton coupling in the radical pair state(s) and (ii) some experimental anomaly may occur in that region (see footnote 3). Similar arguments hold for the 599 nm bleaching band which should represent both the bleaching of the Q_x bands of P and B_A if the first intermediate was P^+B^-HQ. We can exclude any experimental anomalies in that region though. We conclude that the overall appearance of the SADS of the first intermediate is generally in good agreement with the assignment by Zinth and co-workers as a P^+B^-HQ state, although there may exist some lack in the size of the bleaching bands at 813 and 599 nm which might however be fully explained by some modified electronic coupling between pigments in that state (Parson & Warshel, 1987). Note that this intermediate state is required in both the forward and the reversible models. We note also that despite some overall agreement there are also some significant and noteworthy differences present between the SADS of the first intermediate (henceforth identified as the P^+B^-HQ state) in Figure 5 and the corresponding spectrum by Holzapfel et al. (1990). For example, at 600 nm, no bleaching occurs in the spectrum of Holzapfel et al. (1990) as compared to the clear bleaching band in panels A and B of Figure 5 for this spectrum. Such spectral differences may be due to the different relative polarizations of pump and probe beams in our work and that of Holzapfel et al. (1990).

The reversible reaction scheme for the first step may thus be considered as a significant correction to the pure forward model. It is well-justified however when considering the earlier results from charge recombination fluorescence which is pronounced. These fluorescence components can only be explained within the same kinetic scheme if the reversible model is applied. Comparison with fluorescence data thus strongly supports some substantial rate for the back-reaction as determined in the reversible model. The further implications for the energetics will be discussed below. For the SADS of intermediate 2, the most pronounced differences between the two models are located at wavelengths between 700 and 800 nm and around 543 nm, i.e. at wavelengths where H is expected to show pronounced spectral features. Both the difference absorption band at 785 nm and, more pronounced, the bleaching band at 760 nm are larger in the reversible model for the second intermediate (Figure 5B) than in the forward model (Figure 5A). Also, the bleaching at 543 nm is stronger in the reversible model. In the forward model, an unexpected irregular band shape appears instead at 760 nm. All these differences are important for a judgment, since these are exactly the locations of the Q_x and Q_y bands of H which should be bleached in the P^+BH^-Q state. Thus, despite the not very dramatic differences, comparison of the SADS for the second intermediate between the two models nevertheless supports the reversible model over the forward model since the SADS of intermediate 2 are in somewhat better agreement with a prospective P^+BH^-Q state than the one for the forward model. Comparison of the spectrum at a 10−20 ps delay (cf. Figure 3) with published spectra (Woodbury et al., 1985; Holten et al., 1980) shows quite good agreement in all wavelength ranges. It has always been surprising, however, why the 760 nm band did not show up as a quite strong bleaching band at a time (>10 and <200 ps) when basically only the P^+BH^-Q state should have been present according to the current understanding. Furthermore, the decay of the small bleaching at 760 nm when going to the P^+BHQ^- state was also rather small (Kirmaier et al., 1985a; Woodbury et al., 1985). These features did not fit well the notion that H has an absorption band at 760 nm which should be bleached upon its reduction. The present spectrum provides some improvement but still does not show all expected features. In this connection, it should be mentioned that intensity redistributions between spectral regions have been predicted on the basis of exciton calculations (Parson & Warshel, 1987).

Figure 6 shows the calculated time courses of the intermediates in the two kinetic models. Due to the substantial reverse rate in the second step, the intermediate concentration of the P^+B^-HQ state is quite high, in a ratio of about 1/6.5 to the P^+BH^-Q state. In fact, a quasi-equilibrium is established between these states that persists from a time longer than 10 ps up to the decay of that equilibrated state into the P^+BHQ^- state, i.e. over a time of several hundred picoseconds. In contrast, in the forward model, the maximal concentration of the P^+B^-HQ state reaches 30% at about 2 ps and at 15 ps has decayed to less than 1%. Thus, above 10 ps, essentially only the P^+BH^-Q state is present in the forward model. Consequently, the result of the modeling for the SADS of the P^+BH^-Q state

[3] Note that the time-resolved spectra may be substantially distorted at 800 ± 7 nm due to the fact that this is the generating wavelength for the white probing light, and consequently, some anomalies may occur in that region.

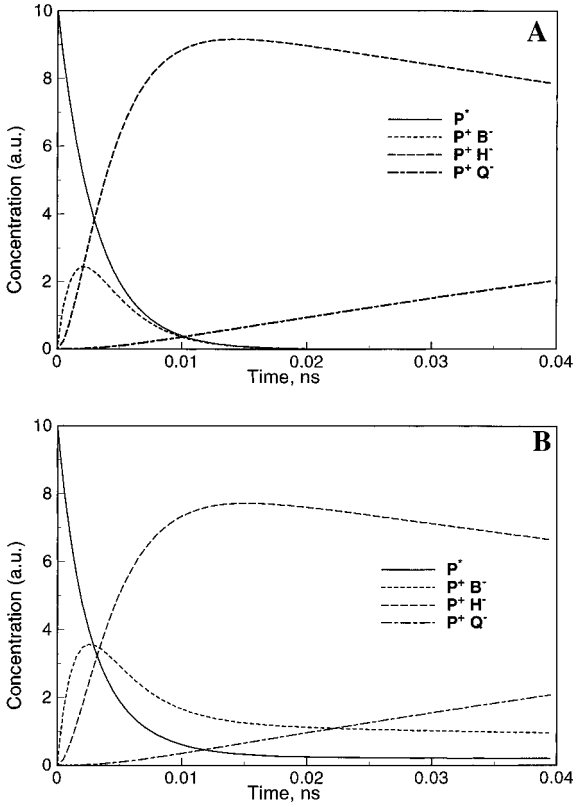

FIGURE 6: Time courses of the concentrations of the various intermediates for the two kinetic models shown in Figure 4.

at 760 nm is a small band only (Figure 5A). In contrast, the reversible model accounts for the presence of the significant percentage of about 15% of the P^+B^-HQ state in the equilibrium. The surprisingly small bleaching at 760 nm at times >10 ps (Figure 3) and the small decay of this bleaching when going to the P^+BHQ^- state is partially explained on the basis of the concentration ratios in the reversible model and the corresponding SADS. The P^+B^-HQ state (strong absorption increase) and the P^+BH^-Q state (absorption decrease) have opposite absorption changes below 760 nm, while the P^+BHQ^- state has essentially no absorption change in that region. Thus, the presence of a substantial amount of the P^+B^-HQ state in the long-living quasi-equilibrium compensates partially for the expected bleaching of the P^+BH^-Q state at and below 760 nm, resulting in a reduced overall bleaching at times between 10 ps and several hundred picoseconds. The pure P^+BH^-Q state in contrast has a quite strong bleaching band at 750 nm (cf Figure 5B) in its difference spectrum to ground state, as would be expected from the general understanding of the difference spectrum of this intermediate. Quite similar arguments can be used for the 543 nm bleaching band of H, although the compensating effect is less pronounced there and for this reason also the spectra at delay times of >10 ps as well as the SADS in the forward model showed already a clear band at this wavelength. However, in the reversible model, the P^+BH^-Q state again has a more pronounced bleaching at 543 nm. Interestingly, a rather symmetric dispersive band shape occurs with a center at 800 nm in the SADS of the P^+BH^-Q state in the reversible model (and somewhat less symmetric also in the forward model) with a negative lobe at 813 nm and a positive lobe at 785 nm. This seems to indicate that both B bands undergo an electrochromic blue shift. This may explain why the bleaching maximum at 813 nm in the P^+B^-HQ state and the P^+BH^-Q state are nearly at the same wavelength (Figure 5B). Interesting and new features of the SADS of the P^+B^-HQ state in the reversible model are also the expected, but so far unobserved, electrochromic shifts in the H bands (Q_x and Q_y) due to the presence of P^+B^-.

The third intermediate should correspond to the nondecaying (on our time scale) P^+BHQ^- state. The corresponding SADS shows the well-known features of this state (Kirmaier et al., 1985a), and the spectra are virtually identical for both kinetic models, which is expected already for formal kinetic reasons.

In summary, we conclude that the reversible model is in very good agreement with the results of spontaneous fluorescence kinetics studies and furthermore gives rise to SADS that are in somewhat better agreement with the expected difference spectra in particular for the P^+BH^-Q state than the pure forward reaction model. Taken together, the reversible model is clearly preferred over the forward model, in particular with respect to the second reaction step. Interestingly, hardly any difference was observed in the SADS of Holzapfel et al. (1990) between the P^+BH^-Q state and the P^+BHQ^- state above 700 nm. Although partly explainable by the different polarizations of pump and probe, this is clearly a consequence of the unsatisfactory description of the time courses of the P^+BH^-Q and the P^+B^-HQ intermediates within the pure forward model (Figure 4A).

Energetics of Radical Pairs. Using equilibrium thermodynamics, we can calculate from the optimal rate constants in the reversible model the free energy differences ΔG between states by using

$$\Delta G = -RT \ln\left(\frac{k_{\text{forw}}}{k_{\text{rev}}}\right)$$

Thus, ΔG values of $\Delta G_1 = -41 \pm 5$ meV and $\Delta G_2 = -50 \pm 6$ meV are obtained for the first and second reaction, respectively. The error ranges have been calculated on the basis of an estimation of an error of ±10% in the rate constants and neglect systematic errors that might be present due to the possible choice of too simple a kinetic model.

The ΔG_1 value determined here for the wild-type RC of −41 meV (−328 cm^{-1}) should be compared with the corresponding value of −450 cm^{-1} determined recently within the framework of a reversible kinetic scheme for a chemically modified RC where the bacteriopheophytins had been replaced by pheophytin *a* (Schmidt et al., 1994). Thus, one may conclude that chemical replacement of H has not changed substantially the energy of the P^+B^- state. Our value for the free energy difference $\Delta G(P^*/P^+BH^-Q) = \Delta G_1 + \Delta G_2 = -91$ meV (−730 cm^{-1}; average values were taken) in contrast is only slightly larger than the −630 cm^{-1} value determined for the chemically modified RC (Schmidt et al., 1994). This is quite surprising even taking into account the error ranges, since the difference in redox potential between BPheo *a* and Pheo *a* of ≈130 meV should have lifted the P^+BH^-Q state in the chemically modified RC by a similar amount relative to the wild-type RC. At present, we have no explanation for this discrepancy, but we note that the results of Shkuropatov and Shuvalov (1993) on a similarly modified RC, suggesting an equilibrium of P^+B^-HQ/P^+BH^-Q in a ratio of 80/20 implies an ≈36 meV higher energy for the P^+BH^-Q state in the chemically modified RC as

compared to that of the P^+B^-HQ state. If compared with our value of $\Delta G_2 = -51$ meV, this implies an increase by about 87 meV of the energy of the P^+BH^-Q state in the Pheo *a*-replaced RC relative to the wild type. This is still not in quantitative agreement with the expectation based on redox potential differences, but the direction and magnitude of change is in better agreement with our data.

A free energy difference $\Delta G(P^*/P^+BH^-Q) = -200$ to -250 meV has been determined by MARY spectroscopy (Ogrodnik et al., 1988, 1994; Ogrodnik, 1990) and direct triplet determination (Goldstein et al., 1988) for the wild-type RC, and this is the value that is widely accepted at present. The free energy difference of -91 ± 10 meV[4] determined here by femtosecond spectroscopy is smaller than that value by at least a factor of 2. These two values are thus at such a vast discrepancy that they cannot be brought into agreement within any reasonable error margins. We have no reason at present to doubt the values of Goldstein et al. (1988) and Ogrodnik et al. (1994). If one takes both values seriously, one must look at the differences in the respective measurements for a possible explanation. Our value of -41 meV measured by femtosecond spectroscopy is determined on the same time scale (≈ 10 ps) as the electron transfer process occurs. In contrast, the ΔG value of Goldstein et al. (1988) and Ogrodnik et al. (1994) is determined after a long time, typically hundreds of nanoseconds to even microseconds. If on such a long time scale a relaxation of the energy of the RP occurs due to protein conformational changes, the seemingly conflicting values could be brought into agreement. Such a picture would in fact be in excellent agreement with results based on charge recombination fluorescence (Müller et al., 1992, 1995; Peloquin et al., 1994). It has always been an unsolved puzzle to explain the discrepancy between the very low free energy differences for the (then assumed pure) P^+BH^-Q state relative to that of P* which was determined from charge recombination fluorescence (Woodbury & Parson, 1984) as compared to the much larger free energy difference based on triplet spectroscopy. So far, the obvious discrepancy has been explained by those who did not accept the radical pair relaxation model in the following way. If the P^+BH^-Q state has a wide static energy distribution (Ogrodnik et al., 1994), then charge recombination fluorescence would detect preferentially such states from the distribution that are high in energy, i.e. charge recombination fluorescence would not look at all the P^+BH^-Q states with equal sensitivity and, more importantly, would be insensitive to the bulk of the RPs (which were assumed to have a low energy). This explanation can, however, now be fully excluded for the transient absorption measurements. We expect that any energy distribution would not have any substantial influence on the difference spectrum of the P^+BH^-Q state. Thus, transient absorption looks at all P^+BH^-Q states with the same sensitivity, and what is determined here as the free energy difference is, even in the presence of some energy distribution for that state, the average free energy difference that should be typical for the bulk of the RCs. It is interesting to compare the free energy difference $\Delta G(P^*/P^+H^-) \approx -55$ meV (for the first discernible RP state in charge recombination, based on a sequential relaxation model with discrete states) as determined by charge recombination fluorescence (Müller et al., 1992) with our value of -41 meV from femtosecond transient absorption. More recent data on this model in a membrane-bound RC (Müller et al., 1995) gave very similar values. Thus, the energy differences determined by these two methods are in excellent agreement and seem to strongly support the conformational cooling model (Müller et al., 1992, 1995). Woodbury and co-workers recently invoked an analogous model (they call it the "dynamic solvation" model) to explain the nonexponentiality of stimulated and spontaneous emission in R26 RCs and two high-redox pontential mutant RCs (Woodbury et al., 1994). Since their measurements have been carried out on Q-reduced RCs, which will presumably modify the energetics of the RPs, their data should probably not be compared to ours in quantitative terms. However, the magnitude and characteristics of the effects reported in their work are in good agreement with our data and support quite similar models. On the basis of the energetics determined here for the wild-type, the initial RP states in the double mutant of Woodbury et al. (1994) should have energies close to or even above that of P* for the unrelaxed RPs. Thus, charge separation might be endothermic in these and also other high-redox potential mutants which would explain many of the so far not understood observed effects, including their slow charge separation rates. We note also that photosystem II RCs show a high charge recombination fluorescence (Gatzen et al., 1996; Roelofs et al., 1991; Crystall et al., 1989; Booth et al., 1991). Thus, for the first time we seem to approach a more quantitative agreement of results based on fluorescence and transient absorption measurements.

Implications for the Understanding of the Electron Transfer Process(es). The data provided here have several consequences for the theoretical understanding of the early electron transfer processes in the RC. We provide evidence for a very small free energy gap of the P^+BH^-Q state to P* on the time scale of the first two electron transfer reactions (-91 meV). The data further provide strong support for the notion that the electron transfer to P^+BH^-Q is followed on a slower time scale by a conformational cooling or relaxation process of the surrounding protein modes which gives rise to (on a sufficiently long time scale of tens to possibly hundreds of nanoseconds) an energetic relaxation of ≥ 150 meV. Thus, a new picture emerges. One may state that in energetic terms the overall charge separation is driven about equally strongly by the protein relaxation as by the initial electron transfer process(es). In any case, the dynamics of the protein must be considered as very essential for the system to function properly. In this connection, the recently reported volume changes of the RCs upon charge separation can be envisaged as a direct consequence of the induced conformational dynamics of the apoprotein upon charge separation (Malkin et al., 1994; Yruela et al., 1994).

Further important consequences follow from the low-energy difference $\Delta G_2 = -50$ meV between the P^+B^-HQ and the P^+BH^-Q states. Firstly, the fact that the two states are present over a long time in an equilibrium influences substantially the spin-dephasing processes in the RPs. The interpretation of, e.g., the MARY experiments (Ogrodnik et al., 1994) as well as other related experiments may have to be revised in light of this new picture. In this connection, it is interesting to note that the small energy difference between the P^+B^-HQ and the P^+BH^-Q states might well explain the

[4] We consider this value as the low limit of the free energy. More refined models may well lead to smaller $|\Delta G|$ values.

previously observed anomaly for the spin-exchange integral of the primary radical pair (Haberkorn et al., 1979) by assigning the P^+B^-HQ state to the postulated "close state". Another explanation for this anomaly, i.e. radical pair relaxation (Goldstein & Boxer, 1989), would also be consistent with our findings. An attractive possibility would be that both of these effects work together simultaneously. Secondly, referring to the consequences of possible energy distributions of the RP state energies, we note that due to the small energy difference in the second step the corresponding rates are in principle as equally susceptible to a dispersive kinetics as those in the first step.

Electron Transfer Parameters. The very small value of $\Delta G_1 = -41$ meV for the first electron transfer step is in reasonable agreement with the reorganization energy λ of $\approx$31 meV ($\approx$250 cm^{-1}) estimated for this reaction from a series of mutants from *Rhodobacter capsulatus* (we prefer here the value of λ determined for the short component only) (Jia et al., 1993). This close agreement, ignoring all possible systematic errors, may be taken as a strong hint that the electron transfer occurs at or very close to the maximum rate in the wild-type RC. We thus equate $\lambda = -\Delta G$ and use the theoretical equations for the electron transfer rate in order to determine V, the electronic coupling matrix element. Using the rate equation of Bixon and Jortner (1989) for the pseudo-activationless case with a medium mode frequency of $\nu = 80$ cm^{-1}, we obtain an optimal value $V_{12} \approx 19$ cm^{-1} for the first ET step. These parameters also provide a very good description of the T dependence of the rate k_{12} (Fleming et al., 1988) (note that at low temperatures the measured lifetime will be a better estimate of the inverse rate k_{12} than at room temperature; see below). Likewise, $V_{23} \approx 20$ cm^{-1} is found to be optimal for the second step. These conditions are clearly favorable for a sequential mechanism with B^- as a real intermediate as originally proposed by Zinth and coworkers on the basis of a pure forward reaction scheme. We note that under these conditions only a very modest rate distribution near the condition $\lambda \approx -\Delta G$ even for a fairly wide distribution in ΔG is predicted by the theory (Bixon & Jortner, 1989). This would be in agreement with our experimental finding of a rather narrow (if any) distribution in the fast rates (or lifetimes). The reorganization energy λ for the first step could be increased in this model without requiring any significant change in the other parameters up to a value of $\leq$380 cm^{-1}. Further increase of λ would lead to a substantial deviation from the proper prediction of T dependence of the rate k_{12} (Fleming et al., 1988).[5] This result is at variance with the presently accepted much larger reorganization energy of $\approx$800 cm^{-1} for the first step (Bixon et al., 1995), while the ΔG value is in very good agreement with the currently assumed values. Thus, the T dependence also indicates that the free energy change and the reorganization energy are optimally matched for the first electron step, and presumably also for the second step.

Some final remarks are in order here. The reversibility of reactions in the preferred kinetic model implies a substantial inherent nonexponentiality in the P* decay without any distribution in the rates being present. The possible presence of any additional nonexponentiality due to a dispersion in one or more of the electron transfer parameters will have to be explored in the future. Furthermore, since all rates for the primary processes are of the same order of magnitude (cf. Figure 4), the observed lifetimes are complex functions of all these rate constants. For example, our lifetime of 1.5 ps cannot be attributed directly to any of the two steps. Thus, any change in a lifetime cannot be simply related to a change in the rate of a particular process. Rather, the full set of rates must be determined from an extended set of high-quality transient absorption data in each case as carried out here. Only then can the molecular rate constants and the free energy differences be determined with sufficient accuracy. This would particularly be relevant when mutants are being studied. For example, in view of the small free energy differences in the first two steps, any increase in P/P^+ redox potential by mutation, besides the possibility of significantly changing more than one rate, will have the effect of increasing the nonexponentiality and changing all fast lifetimes even without any change in one of the forward reaction rates. Thus, in this situation, the direct use of either a measured single or average lifetime in a rate expression for deducing electron transfer parameters λ, V, etc., as has been done in the past, will likely cause some substantial systematic errors.

[5] Note that the actual increase in the rate constant for the first step when going from room temperature to 4 K is only a factor of 2, i.e. from the $(2.48\ ps)^{-1}$ determined here to about $(1.2\ ps)^{-1}$ at low T.

ACKNOWLEDGMENT

We thank Mrs. I. Martin for development of the data analysis programs and Mr. M. Reus for preparing the reaction centers. We also thank Prof. K. Schaffner for support of this work.

REFERENCES

Alden, R. G., Parson, W. W., Chu, Z. T., & Warshel, A. (1995) *J. Am. Chem. Soc. 117*, 12284.
Arlt, T., Schmidt, S., Kaiser, W., Lauterwasser, C., Meyer, M., Scheer, H., & Zinth, W. (1993) *Proc. Natl. Acad. Sci. USA 90*, 11757.
Bixon, M., Jortner, J., & Michel-Beyerle, M. E. (1995) *Chem. Phys. 197*, 389.
Bixon, M., & Jortner, J. (1989) *Chem. Phys. Lett. 159*, 17.
Booth, P. J., Crystall, B., Giorgi, L. B., Barber, J., Klug, D. R., & Porter, G. (1990) *Biochim. Biophys. Acta 1016*, 141.
Booth, P. J., Crystall, B., Ahmad, I., Barber, J., Porter, G., & Klug, D. R. (1991) *Biochemistry 30*, 7573.
Boxer, S. G., Goldstein, R. A., Lockhart, D. J., Middendorf, T. R., & Takiff, L. (1988) in *The Photosynthetic Bacterial Reaction Center. NATO ASI Series Vol.149* (Breton, J., & Vermeglio, A., Eds.) pp 165−176, Plenum Press, New York.
Chidsey, C. E. D., Takiff, L., Goldstein, R. A., & Boxer, S. G. (1985) *Proc. Natl. Acad. Sci. USA 82*, 6850.
Creighton, S., Hwang, J.-K., Warshel, A., Parson, W. W., & Norris, J. (1988) *Biochemistry 27*, 774.
Crystall, B., Booth, P. J., Klug, D. R., Barber, J., & Porter, G. (1989) *FEBS Lett. 249*, 75.
Du, M., Rosenthal, S. J., Xie, X. L., Dimagno, T. J., Schmidt, M., Hanson, D. K., Schiffer, M., Norris, J. R., & Fleming, G. R. (1992) *Proc. Natl. Acad. Sci. USA 89*, 8517.
Fleming, G. R., Martin, J.-L., & Breton, J. (1988) *Nature 333*, 190.
Gatzen, G., Müller, M. G., Griebenow, K., & Holzwarth, A. R. (1996) *J. Phys. Chem. 100*, 7269.
Goldstein, R. A., Takiff, L., & Boxer, S. G. (1988) *Biochim. Biophys. Acta 934*, 253.
Goldstein, R. A., & Boxer, S. G. (1989) *Biochim. Biophys. Acta 977*, 78.
Haberkorn, R., Michel-Beyerle, M. E., & Marcus, R. A. (1979) *Proc. Natl. Acad. Sci. USA 76*, 4185.
Hamm, P., Gray, K. A., Oesterhelt, D., Feick, R., Scheer, H., & Zinth, W. (1993) *Biochim. Biophys. Acta 1142*, 99.

Holten, D., Hoganson, C., Windsor, M. W., Schenck, C. C., Parson, W. W., Migus, M. W., Fork, R. L., & Shank, C. V. (1980) *Biochim. Biophys. Acta 592*, 461.
Holzapfel, W., Finkele, U., Kaiser, W., Oesterhelt, D., Scheer, H., Stilz, H. U., & Zinth, W. (1989) *Chem. Phys. Lett. 160*, 1.
Holzapfel, W., Finkele, U., Kaiser, W., Oesterhelt, D., Scheer, H., Stilz, H. U., & Zinth, W. (1990) *Proc. Natl. Acad. Sci. USA 87*, 5168.
Holzwarth, A. R., Schatz, G. H., Brock, H., & Bittersmann, E. (1993) *Biophys. J. 64*, 1813.
Holzwarth, A. R. (1996) in *Biophysical Techniques. Advances in Photosynthesis Research* (Amesz, J., & Hoff, A., Eds.) pp 75−92, Kluwer Academic Publishers, Dordrecht.
Horber, J. K. H., Göbel, W., Ogrodnik, A., Michel-Beyerle, M. E., & Cogdell, R. J. (1986) *FEBS Lett. 198*, 273.
Jia, Y. W., Dimagno, T. J., Chan, C. K., Wang, Z. Y., Du, M., Hanson, D. K., Norris, J. R., Fleming, G. R., & Popov, M. S. (1993) *J. Phys. Chem. 97*, 13180.
Kirmaier, C., Holten, D., & Parson, W. W. (1985a) *Biochim. Biophys. Acta 810*, 33.
Kirmaier, C., Holten, D., & Parson, W. W. (1985b) *FEBS Lett. 185*, 76.
Kirmaier, C., & Holten, D. (1990) *Proc. Natl. Acad. Sci. USA 87*, 3552.
Kirmaier, C., & Holten, D. (1991) *Biochemistry 30*, 609.
Konermann, L., Gatzen, G., & Holzwarth, A. R. (1996) *J. Phys. Chem.* (in press)
Malkin, S., Churio, M. S., Braslavsky, S. E., & Shochat, S. (1994) *J. Photochem. Photobiol. B 23*, 79.
Marcus, R. A. (1987) *Chem. Phys. Lett. 133*, 471.
Moser, C. C., Keske, J. M., Warncke, K., Farid, R. S., & Dutton, P. L. (1993) in *The Photosynthetic Reaction Center. II* (Deisenhofer, J., & Norris, J. R., Eds.) pp 1−22, Academic Press, San Diego.
Müller, M. G., Griebenow, K., & Holzwarth, A. R. (1991) *Biochim. Biophys. Acta 1098*, 1.
Müller, M. G., Griebenow, K., & Holzwarth, A. R. (1992) *Chem. Phys. Lett. 199*, 465.
Müller, M. G., Drews, G., & Holzwarth, A. R. (1993) *Biochim. Biophys. Acta 1142*, 49.
Müller, M. G., Dorra, D., Holzwarth, A. R., Gad'on, N., & Drews, G. (1995) in *Photosynthesis: from Light to Biosphere. Vol.I. Proc. of the Xth International Photosynthesis Congress. Montpellier 1995* (Mathis, P., Ed.) pp 595−598, Kluwer Academic Publishers, Dordrecht.
Müller, M. G., Hucke, M., Reus, M., & Holzwarth, A. R. (1996) *J. Phys. Chem. 100*, 9527.
Ogrodnik, A., Volk, M., Letterer, R., Feick, R., & Michel-Beyerle, M. E. (1988) *Biochim. Biophys. Acta 936*, 361.
Ogrodnik, A. (1990) *Biochim. Biophys. Acta 1020*, 65.
Ogrodnik, A., Keupp, W., Volk, M., Aumeier, G., & Michel-Beyerle, M. E. (1994) *J. Phys. Chem. 98*, 3432.
Parson, W. W., Chu, Z.-T., & Warshel, A. (1990) *Biochim. Biophys. Acta 1017*, 251.
Parson, W. W. (1991) in *Chlorophylls* (Scheer, H., Ed.) pp 1153−1180, CRC Press, Boca Raton.
Parson, W. W., & Warshel, A. (1987) *J. Am. Chem. Soc. 109*, 6152.
Peloquin, J. M., Williams, J. C., Lin, X., Alden, R. G., Taguchi, A. K. W., Allen, J. P., & Woodbury, N. W. (1994) *Biochemistry 33*, 8089.
Roelofs, T. A., Gilbert, M., Shuvalov, V. A., & Holzwarth, A. R. (1991) *Biochim. Biophys. Acta 1060*, 237.
Schmidt, S., Arlt, T., Hamm, P., Huber, H., Nagele, T., Wachtveitl, J., Meyer, M., Scheer, H., & Zinth, W. (1994) *Chem. Phys. Lett. 223*, 116.
Shkuropatov, A. Y., & Shuvalov, V. A. (1993) *FEBS Lett. 322*, 168.
Skourtis, S. S., da Silva, A. J. R., Bialek, W., & Onuchic, J. N. (1992) *J. Phys. Chem. 96*, 8034.
Vos, M. H., Lambry, J.-C., Robles, S. J., Youvan, D. C., Breton, J., & Martin, J.-L. (1991) *Proc. Natl. Acad. Sci. USA 88*, 8885.
Vos, M. H., Jones, M. R., Hunter, C. N., Breton, J., & Martin, J.-L. (1994) *Proc. Natl. Acad. Sci. USA 91*, 12701.
Wang, Z. Y., Pearlstein, R. M., Jia, Y. W., Fleming, G. R., & Norris, J. R. (1993) *Chem. Phys. 176*, 421.
Woodbury, N. W., Becker, M., Middendorf, D., & Parson, W. W. (1985) *Biochemistry 24*, 7516.
Woodbury, N. W., Peloquin, J. M., Alden, R. G., Lin, X., Lin, S., Taguchi, A. K. W., Williams, J. C., & Allen, J. P. (1994) *Biochemistry 33*, 8101.
Woodbury, N. W., & Parson, W. W. (1986) *Biochim. Biophys. Acta 850*, 197.
Woodbury, N. W. T., & Parson, W. W. (1984) *Biochim. Biophys. Acta 767*, 345.
Yruela, I., Churio, M. S., Gensch, T., Braslavsky, S. E., & Holzwarth, A. R. (1994) *J. Phys. Chem. 98*, 12789.

BI9607012